Author/s:
Richard, D;MacRaild, CA;Riglar, DT;Chan, JA;Foley, M;Baum, J;Ralph, SA;Norton, RS;Cowman, AF

Title:
Interaction between Plasmodium falciparum apical membrane antigen 1 and the rhoptry neck protein complex defines a key step in the erythrocyte invasion process of malaria parasites

Date:
2010-05-07

Citation:
Richard, D., MacRaild, C. A., Riglar, D. T., Chan, J. A., Foley, M., Baum, J., Ralph, S. A., Norton, R. S. & Cowman, A. F. (2010). Interaction between Plasmodium falciparum apical membrane antigen 1 and the rhoptry neck protein complex defines a key step in the erythrocyte invasion process of malaria parasites. Journal of Biological Chemistry, 285 (19), pp.14815-14822. https://doi.org/10.1074/jbc.M109.080770.

Persistent Link:
https://hdl.handle.net/11343/263795

⌘ *Author's Choice*

THE JOURNAL OF BIOLOGICAL CHEMISTRY VOL. 285, NO. 19, pp. 14815–14822, May 7, 2010

Interaction between *Plasmodium falciparum* Apical Membrane Antigen 1 and the Rhoptry Neck Protein Complex Defines a Key Step in the Erythrocyte Invasion Process of Malaria Parasites*[S]

Received for publication, October 30, 2009, and in revised form, February 24, 2010 Published, JBC Papers in Press, March 12, 2010, DOI 10.1074/jbc.M109.080770

Dave Richard[‡1], Christopher A. MacRaild[‡], David T. Riglar[‡], Jo-Anne Chan[‡], Michael Foley[§], Jake Baum[‡], Stuart A. Ralph[¶], Raymond S. Norton[‡2], and Alan F. Cowman[‡3]

From the [‡]Walter and Eliza Hall Institute of Medical Research, Parkville, Melbourne, Victoria 3052, the [§]Department of Biochemistry, La Trobe University, Bundoora, Victoria 3086, and the [¶]Bio21 Molecular Sciences and Biotechnology Institute, University of Melbourne, Melbourne, Victoria 3010, Australia

Invasion of host cells by apicomplexan parasites, including *Plasmodium falciparum* and *Toxoplasma gondii*, is a multistep process. Central to invasion is the formation of a tight junction, an aperture in the host cell through which the parasite pulls itself before settling into a newly formed parasitophorous vacuole. Two protein groups, derived from different secretory organelles, the micronemal protein AMA1 and the rhoptry proteins RON2, RON4, and RON5, have been shown to form part of this structure, with antibodies targeting *P. falciparum* AMA1 known to inhibit invasion, probably via disruption of its association with the PfRON proteins. Inhibitory AMA1-binding peptides have also been described that block *P. falciparum* merozoite invasion of the erythrocyte. One of these, R1, blocks invasion some time after initial attachment to the erythrocyte and reorientation of the merozoite to its apical pole. Here we show that the R1 peptide binds the PfAMA1 hydrophobic trough and demonstrate that binding to this region prevents its interaction with the PfRON complex. We show that this defined association between PfAMA1 and the PfRON complex occurs after reorientation and engagement of the actomyosin motor and argue that it precedes rhoptry release. We propose that the formation of the AMA1-RON complex is essential for secretion of the rhoptry contents, which then allows the establishment of parasite infection within the parasitophorous vacuole.

Apicomplexan parasites are an ancient phylum of protozoan parasites, several members of which are important pathogens of humans, including *Toxoplasma gondii* and the malaria parasite *Plasmodium falciparum*. All Apicomplexa are obligate intracellular parasites that invade a host cell at some point in their lifecycle to complete development. Indeed, the defining feature of this phylum is the presence, in the motile parasite form, of an apical complex composed of secretory organelles termed micronemes, rhoptries, and dense granules. The process of host cell invasion involves a series of tightly regulated steps. After initial contact of the parasite with a target cell, reorientation occurs, resulting in direct juxtaposition of its apical end with the host cell membrane, leading to the formation of a tight junction. This is an irreversible zone of contact where the host and parasite plasma membranes are brought together through interaction of parasite ligands with specific host cell receptors. As invasion proceeds, the junction moves along the parasite to the posterior, powered by an internal actomyosin motor, eventually leading to a fusion of the erythrocyte membrane with release of the parasite into a parasitophorous vacuole surrounded by the parasitophorous vacuole membrane inside the host cell (1).

The invasive blood stage form of *P. falciparum*, the merozoite, enters the host red cell in less than 30 s (2, 3). Electron microscopy studies of this event have provided a morphologically detailed description of tight junction formation (4, 5), hinting at both the ultrastructure of the junction and the shedding of merozoite surface proteins (6). Recent work has identified likely proteases responsible for this process of shedding and also provided a potential mechanism for disengagement of adhesin-receptor complexes at the junction, an event required for entry of the parasite into the host cell (7). Initial contact of the merozoite with the erythrocyte is a low affinity interaction, most likely involving glycosylphosphatidylinositol-anchored proteins located on the parasite surface (8, 9). Other proteins, such as the micronemal protein apical membrane antigen-1 (PfAMA1),[4] are released onto the surface at or just before merozoite egress and play an essential role in invasion (10), possibly mediating merozoite reorientation following attachment (11). Tight junction formation is thought to occur after reorienta-

* This work was supported by the National Health and Medical Research Council of Australia (NHMRC). This work was supported by an NHMRC Institutes Infrastructure Support Scheme grant and a Victorian State Government Operational Infrastructure Support grant.

⌘ *Author's Choice*—Final version full access.

[S] The on-line version of this article (available at http://www.jbc.org) contains supplemental Figs. 1 and 2 and two movies.

[1] Recipient of a Canadian Institutes of Health Research (CIHR) fellowship.

[2] A Principal Research Fellow of the NHMRC. To whom correspondence may be addressed: The Walter and Eliza Hall Institute of Medical Research, 1G Royal Parade, Parkville, Melbourne, Victoria 3052, Australia. Tel.: 61-3-93452446; Fax: 61-3-93470852; E-mail: rnorton@wehi.edu.au.

[3] A Howard Hughes International Scholar and an Australia Fellow of the NHMRC. To whom correspondence may be addressed: The Walter and Eliza Hall Institute of Medical Research, 1G Royal Parade, Parkville, Melbourne, Victoria 3052, Australia. Tel.: 61-3-93452446; Fax: 61-3-93470852; E-mail: cowman@wehi.edu.au.

[4] The abbreviations used are: PfAMA1, *P. falciparum* apical membrane antigen-1; TgAMA1, *T. gondii* AMA1; HSQC, heteronuclear single quantum correlation.

tion, but little is known about the mechanism that underlies its formation or its molecular architecture.

Recently, a rhoptry neck protein called TgRON4 was shown to localize to the tight junction during invasion of *T. gondii* tachyzoites into mammalian host cells (12, 13). The *T. gondii* orthologue of PfAMA1 (TgAMA1), a micronemal protein, interacts with TgRON4 and two other rhoptry neck proteins, TgRON2 and TgRON5, at the tight junction of tachyzoites during invasion (13). The *P. falciparum* homologues of these proteins have been identified and associate in schizont stage protein extracts, although the apparent composition of the complex has varied between studies (14–17). Although antibodies to PfAMA1 have long been known to inhibit merozoite invasion, the mechanism of inhibition has remained elusive (18). Recently, it has been demonstrated that an invasion inhibitory monoclonal antibody that binds an epitope adjacent to the conserved PfAMA1 hydrophobic pocket prevented its association with the RON complex, suggesting a critical role for this interaction in the invasion process (16). Additional evidence for the role of PfAMA1 has come from studies using a binding peptide, R1, which has been shown to inhibit invasion (19, 20). Live videomicroscopy of merozoites in the presence of R1 peptide showed that they undergo successful reorientation and attachment to the erythrocyte surface, including forceful pulling, but fail to proceed to invasion (21). This suggests that PfAMA1 plays a key role in the transition between attachment and activation of the invasion event, perhaps concurrent with tight junction formation.

To better understand the mechanisms underlying erythrocyte invasion by the malaria parasite *P. falciparum*, we undertook an investigation of how R1 inhibits invasion. Here we demonstrate that R1 binds the PfAMA1 hydrophobic trough and that this prevents the interaction of PfAMA1 with the PfRON complex. Combined with videomicroscopy of R1-inhibited merozoites attempting invasion of erythrocytes, our data provide direct mechanistic insight into this crucial step in the establishment of blood stage infection.

EXPERIMENTAL PROCEDURES

Parasite Cultures—P. falciparum asexual stage parasites were maintained in human erythrocytes (blood group O+) at a hematocrit of 4% with 10% (w/v) Albumax™ (Invitrogen) (22). *P. falciparum* 3D7 parasites were originally obtained from David Walliker at Edinburgh University. Cultures were synchronized as described previously (23).

NMR Spectroscopy—The ectodomain of PfAMA1 (3D7 strain, residues 97–544) was expressed in *Escherichia coli* with an N-terminal His_6 tag and purified and refolded as described previously (24). Recombinant PfAMA1 was specifically ^{13}C-labeled at methionine methyl groups by growth of expression cultures in M9 minimal medium supplemented with 0.15 g liter^{-1} [^{13}C]methyl L-methionine (Sigma) and additional amino acids and metabolites as described (25). Expression plasmids encoding PfAMA1 with each of the point mutations M190I, M198L, M224L, M273L, and M374L were prepared by QuikChange site-directed mutagenesis (Stratagene). NMR experiments were performed using a Bruker Avance 500 spectrometer equipped with a Triple Resonance Inverse (TXI) cryoprobe. Samples were prepared by dissolving lyophilized PfAMA1 in ^2H_2O containing 20 mM sodium phosphate buffer, pH 7.2, 0.03% sodium azide, and Complete protease inhibitor mixture (Roche Applied Science). PfAMA1 concentrations were typically 0.1 mM. Synthetic R1 peptide (GL Biochem) was titrated into PfAMA1 samples from a 2 mM stock in the same buffer.

Antisera—Rabbit and mouse antibodies were raised against $PfRON4_{437-661}$ and $PfRON5_{91-195}$ from glutathione *S*-transferase fusion proteins expressed from plasmid constructs using the following primers: PfRON4F (5′-CGCGGATCCCCAACGAATGAACCTATTCC-3′); PfRON4R (5′-CCGCTCGAGACATGATTTCCTCCTACTGG-3′); PfRON5F (5′-CGCGGATCCATACCTGACCCAGGAGATG-3′); and PfRON5R (5′-CCGCTCGAGTTCTTTACTTTTCTCGATAG-3′). PCR products were digested with BamHI/XhoI (underlined letters in primers), purified, and cloned into the plasmid pGEX4T-1 (Amersham Biosciences). For immunoblots, saponin-lysed parasite pellets from highly synchronous schizont 3D7 parasites as well as culture supernatants (post-schizont rupture/reinvasion) were separated in sample buffer on 4–12% (w/v) SDS-NuPAGE gels (Invitrogen) under reducing conditions and transferred to nitrocellulose membranes (Schleicher & Schuell). Rabbit and mouse antisera were diluted in 0.1% (v/v) Tween 20-phosphate-buffered saline with 1% (w/v) skim milk. Appropriate secondary antibodies were used, and immunoblots were developed by ECL (Amersham Biosciences).

Fluorescence Imaging—Fluorescence images of schizont stage parasites were captured using a Carl Zeiss Axioskop microscope with a PCO Sensicam and Axiovision 2 software. For immunofluorescence assays of free and/or invading merozoites, highly synchronous schizont stage 3D7 parasites in the process of rupture/reinvasion were smeared and fixed in 100% methanol at −20 °C. After blocking in 3% (w/v) bovine serum albumin (Sigma), the cells were incubated for 1 h with the appropriate antisera: rabbit anti-PfRON4 (1/200), mouse monoclonal anti-PfRON4 (1/200), mouse monoclonal anti-PfRON5 (1/50), mouse monoclonal anti-PfRAP1 (1/500), rabbit anti-PfRAMA (1/200) (26), and rabbit polyclonal anti-AMA1 (1/500) (27). Bound antibodies were then visualized with Alexa Fluor 488/594 anti-rabbit IgG or anti-mouse IgG (Molecular Probes) diluted 1:1000. Parasites were mounted in VECTASHIELD (Vector Laboratories) containing 4′,6-diamidino-2-phenylindole; Roche Molecular Biochemicals).

Immunoelectron Microscopy—Parasites for electron microscopy immunolabeling were fixed and prepared as described previously (28). The primary antibodies used were mouse monoclonal anti-PfRAP1 and rabbit anti-PfRON4. Samples were washed and then incubated with secondary antibodies conjugated to either 10-nm or 15-nm colloidal gold (BB International). Samples were then post-stained with 2% aqueous uranyl acetate and then 5% triple lead and observed at 120 kV on a Philips CM120 BioTWIN transmission electron microscope.

Immunoprecipitation—Schizont stage proteins were extracted as described previously (33) in 1-ml volumes of 1% T-NET (1% (v/v) Triton X-100, 50 mM Tris-HCl, pH 7.4, 150 mM NaCl, 5 mM EDTA) with Complete protease inhibitor.

Immunoprecipitations were performed using mouse monoclonal antibodies against PfRON4 and rabbit polyclonal antibodies against PfAMA1 with protein G-Sepharose (Amersham Biosciences). For the peptide competition assays, parasites were extracted in lysis buffer containing increasing concentrations of one of the following peptides: R1, an unrelated 20-mer (X1) (Auspep), F1, or F1s (an analogue of F1 with the sequence scrambled) (Auspep); immunoprecipitation was then carried on as usual. Proteins were separated by SDS-PAGE and visualized by Western blot with mouse or rabbit antibodies against PfRON4, PfRON5, and PfAMA1.

Time-lapse Microscopy—Late trophozoite and schizont stage parasites were purified from synchronous culture by passing through a magnetic separation column (MACS Miltenyi Biotec) and resuspended at ~30% parasitemia in ~0.01% hematocrit complete culture medium in FluoroDish culture dishes with cover glass bottoms (World Precision Instruments). Invading parasites were observed using an inverted wide field microscope (Zeiss Axiovert 200 M, Zeiss) using a 100× oil immersion lens (NA 1.40, Zeiss) while at 37 °C and under humidified CO_2 (5%) conditions. Differential interference contrast images were acquired at ~3 frames per second using illumination from a halogen lamp. The supplemental movies were processed using Image J and Adobe PhotoShop CS4 (Adobe) software programs.

RESULTS

The R1 Invasion Inhibitory Peptide Binds the PfAMA1 Hydrophobic Groove—To characterize the interaction between PfAMA1 and R1, we have used NMR spectroscopy. Initial studies with uniformly ^{15}N- or ^{13}C-labeled PfAMA1 ectodomain (residues 97–544) gave poor spectra, with significant line broadening and extensive peak overlap preventing detailed spectral analysis. Despite this, we noted several well resolved methyl resonances in ^{1}H-^{13}C HSQC spectra, a number of which were perturbed upon titration with the R1 peptide. Among the best resolved of these perturbed methyl resonances were peaks with chemical shifts characteristic of methionine methyl groups. We therefore chose to use these methionine methyl resonances as probes to further characterize the interaction of R1 with PfAMA1. The addition of a small molar excess of R1 with PfAMA1, specifically ^{13}C-labeled at Met methyl groups, caused perturbation of five well resolved peaks (Fig. 1*A*), demonstrating that the interaction of R1 with PfAMA1 alters the chemical environment of at least 5 Met residues in AMA1. Of the 11 Met residues in the PfAMA1 ectodomain construct used in these experiments, 6 are present in or near the hydrophobic groove, and the remaining 5 are located at the opposite end of the molecule in and around domain III (Fig. 1*B*).

Spectroscopic assignment of the perturbed peaks was precluded by poor spectral quality, so we attempted to assign them by mutagenesis. Five conservative point mutations of methionine residues near the hydrophobic trough were generated. Of these mutated residues, 3 (Met-190, Met-198, and Met-224) form part of a cluster of 4 methionine residues lying at one end of the hydrophobic trough, whereas Met-273 is located at the opposite end of the trough and Met-374 is located just to one side (Fig. 1*B*). Each PfAMA1 ectodomain methionine mutant

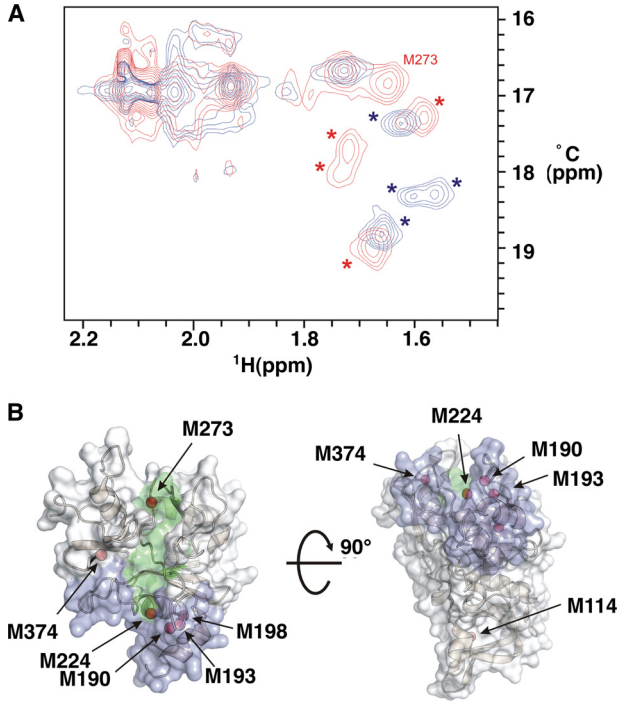

FIGURE 1. **The R1 invasion inhibitory peptide binds the AMA1 hydrophobic groove.** *A*, ^{1}H-^{13}C HSQC of [^{13}C]methyl L-methionine labeled PfAMA1 ectodomain in the presence (*red*) and absence (*blue*) of a molar excess of R1. The peak assigned as the Met-273 methyl resonance is labeled, and the peaks corresponding to the cluster of methionine residues (Met-224, Met-190, Met-193, Met-189) are marked with *asterisks*. *B*, domains I and II of PfAMA1 (PDB code 1Z40), showing the location of methionine methyl groups (*red spheres*), the hydrophobic trough (*green*), and the 1F9 epitope (*blue*). Four additional methionine residues present in domain III are not shown. The figure was prepared with PyMOL (DeLano Scientific).

was ^{13}C-labeled at the remaining methionine methyl groups and confirmed to be correctly folded, as judged by one-dimensional ^{1}H NMR. Despite the conservative nature of the mutations made in each case, we observed significant differences in the ^{1}H-^{13}C HSQC spectra of the M190I, M198L, and M224L mutants, as compared with that of wild-type PfAMA1 (supplemental Fig. 1). These differences prevented specific assignment of the corresponding residues. Nonetheless, we noted a consistent set of well resolved peaks perturbed by mutation of each of these residues, both in the presence and in the absence of R1. This suggests that these perturbations arise from the effect of the mutations on adjacent methyl groups within this cluster of methionine residues. Thus, although residue-specific assignment of these peaks was not possible, we can attribute them to the cluster composed of Met-190, Met-193, Met-198, and Met-224. Importantly, this set of peaks coincides partially with the set of peaks perturbed by R1 (Fig. 1*A*), indicating that the interaction of R1 with PfAMA1 perturbs the cluster of methionine residues at the end of the hydrophobic trough.

The ^{1}H-^{13}C HSQC spectrum (in the presence of an excess of R1) of the M273L mutant was identical to that of wild-type PfAMA1 in the presence of R1, except that a single peak was absent from its spectrum. This assigns the missing peak directly to that of the Met-273 methyl group (supplemental Fig. 1). In the absence of R1, the ^{1}H-^{13}C HSQC spectra of both wild-type and M273L PfAMA1 are similar, showing no alterations in the mutant spectrum. This suggests that in this state, the Met-273

methyl peak is not resolved. Nonetheless, the Met-273 methyl resonance clearly undergoes a marked change in chemical shift as a result of R1 binding. This directly implicates Met-273 in interactions with the R1 peptide (Fig. 1*A*). The ^{1}H-^{13}C HSQC spectrum of M374L PfAMA1 is identical to that of wild type, both in the presence and in the absence of R1, indicating that the corresponding peak is not resolved in either state. This may be due to exchange broadening of this resonance or, more likely, peak overlap with the group of intense peaks with ^{13}C chemical shifts around 17 ppm.

These data demonstrate that the binding site of R1 to PfAMA1 spans the full length of the hydrophobic trough, from Met-273 at one end to the cluster of methionine residues at the other. These sites coincide with the epitopes of two invasion inhibitory monoclonal antibodies, with the cluster of methionine residues closely associated with the epitope of 1F9 (29) and Met-273 lying adjacent to the epitope of 4G2 (30). Both 1F9 and 4G2 are known to compete with R1 for PfAMA1 binding (19). Together, these observations confirm the importance of the hydrophobic trough in the function of PfAMA1 and as a target for inhibitory molecules.

The P. falciparum Homologues of the T. gondii Tight Junction Proteins RON4 and RON5 Localize to the Apical End of the Merozoite and Form a Complex with PfAMA1 in Schizont Protein Extracts—To investigate the effect of R1 on the different components of the *P. falciparum* tight junction, we generated antisera against the PfRON proteins. The *P. falciparum* TgRON4 homologue, PfRON4 (PF11_0168), has a signal peptide but no transmembrane domain and contains a series of repeats, rich in proline and glutamic acid, in its N-terminal region. Immunoblot analysis using antisera raised against a fragment of PfRON4 detected a single band of ~200 kDa (Fig. 2*A*), consistent with data published previously (14, 17). The discrepancy in predicted molecular mass (134 kDa) as compared with that observed (~200 kDa) can most likely be explained by the presence of a high number of repetitive sequences in the N terminus, which are known to affect the mobility of proteins on SDS-PAGE (31). The *P. falciparum* TgRON5 homologue, PfRON5 (MAL8P1.73), has a putative signal sequence at the N terminus, and analysis of its hydrophobicity profile reveals six potential transmembrane regions distributed along the protein. A monoclonal antibody raised to the N terminus of PfRON5 detected a protein band of ~120 kDa, consistent with the predicted size (Fig. 2*A*).

We used specific anti-PfRON antibodies to determine the localization of PfRON4 and PfRON5 in free merozoites. Antibodies to PfRON4 (Fig. 2*B*, *panel a*) and PfRON5 (Fig. 2*B*, *panel b*) showed a single dot at the apical tip of merozoites, in close proximity but never strongly overlapping with the rhoptry bulb markers PfRAP1 (32) and PfRAMA (26), suggesting that they were present in the neck of this organelle, consistent with the localization of PfRON4 determined previously (14). To more finely localize the PfRON proteins in merozoites, we used immunoelectron microscopy. PfRON4 localized to the rhoptry neck, in contrast to PfRAP1, which is present in the body of the bulb (33, 34). Interestingly, PfRON4 was present at the back of the rhoptry neck rather than the front, defined by more electron dense material suggesting a distinct subcompartment (Fig. 2*C*).

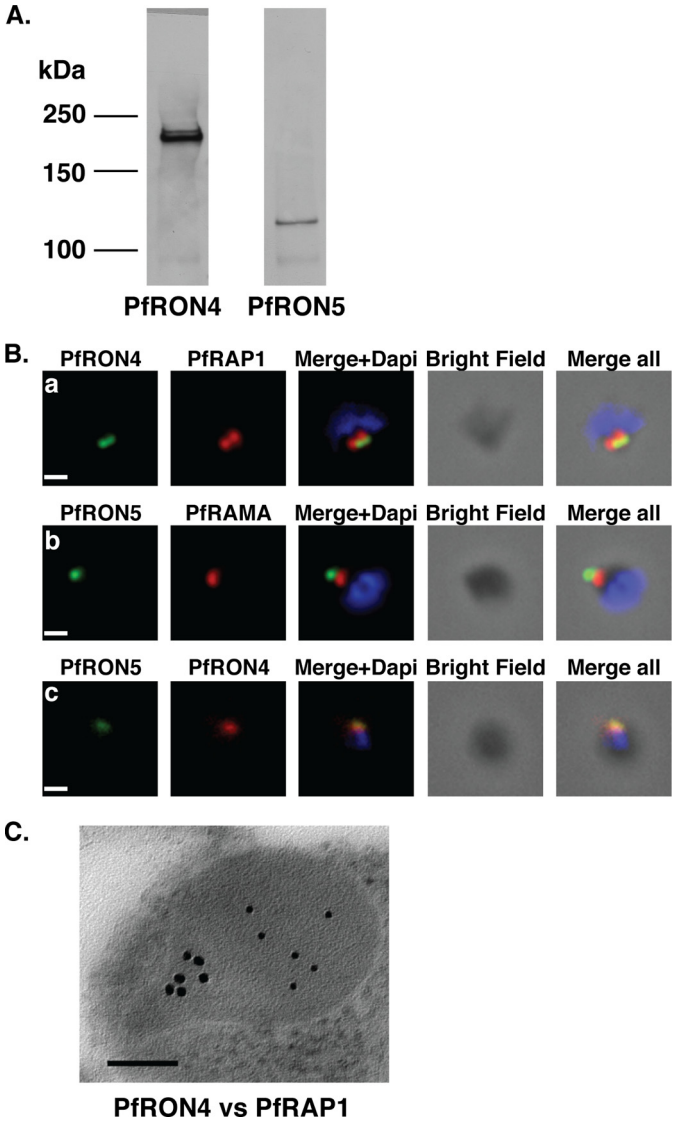

FIGURE 2. **The PfRON4 and PfRON5 proteins localize to the rhoptry neck.** *A*, antibodies raised against PfRON4 and PfRON5 recognize specific protein products in schizont parasite extracts. *B*, immunofluorescence assays using the anti-PfRON antibodies reveal staining of the apical tip of free merozoite, in close apposition with the rhoptry bulb markers PfRAP1 and PfRAMA, suggesting a rhoptry neck localization. *Scale bar*: 0.2 μm. *C*, immunoelectron microscopy confirms that PfRON4 localizes to the rhoptry neck. *Scale bar*: 0.1 μm.

Our attempts to localize PfRON5 by immunoelectron microscopy were not successful; however, co-localization with PfRON4 by immunofluorescence microscopy suggests that PfRON5 co-localizes at the back of the rhoptry neck (Fig. 2*B*, *panel c*). Taken together, these data show that the PfRON proteins are compartmentalized within the rhoptry neck in merozoite stages prior to erythrocyte invasion.

In invading *T. gondii* tachyzoites, TgRON2, TgRON4, and TgRON5 form a complex with the microneme protein TgAMA1 at the moving junction (13). The TgAMA1 association was also observed in free tachyzoites, where the TgRON proteins are in a different cellular compartment from TgAMA1. This is probably the result of TgRON4-TgAMA1 association in solution following cell lysis (13). In the case of *P. falciparum*, conflicting data have been published as to the composition of the tight junction, the only constant being the

association of PfAMA1 with PfRON4 (14, 15, 17). To address the composition of the tight junction complex in *P. falciparum* with respect to specific PfRON antibodies, we performed immunoprecipitation with the anti-PfRON4 and probed the eluates by immunoblot. As expected, anti-PfRON4 antibodies specifically detect a 200-kDa band (Fig. 3, *left panel*). PfRON5 antibodies detect a 120-kDa band of the expected size, confirming that PfRON5 associates with PfRON4 in schizonts (Fig. 3, *middle panel*) Immunoprecipitation with anti-PfRON4 antibodies was used to determine whether PfAMA1 was present in the PfRON complex. The sample was run under non-reducing conditions and probed with an anti-PfAMA1 antibody (27). Full-length 83-kDa and processed 66-kDa forms of PfAMA1 were efficiently co-precipitated with anti-RON4 antibodies, confirming that this protein can form a complex with PfRON4 and PfRON5 (Fig. 3, *right panel*).

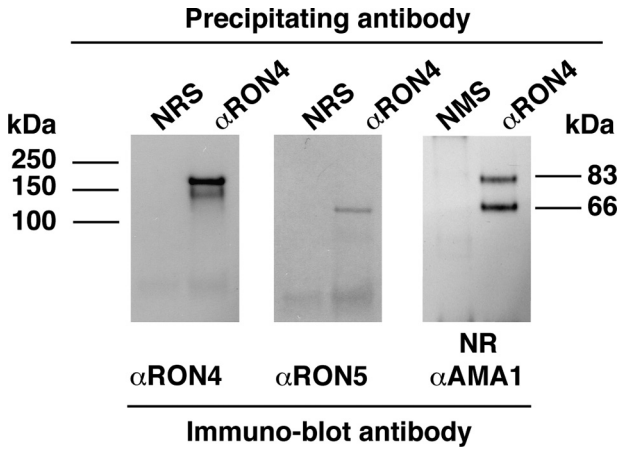

FIGURE 3. **The PfRON4 and PfRON5 proteins form a complex with PfAMA1 in schizonts.** Immunoprecipitation using the anti-PfRON4 probed by Western blot with antibodies against the different PfRONs and PfAMA1 is shown. *NRS*, normal rabbit serum; *NMS*, normal mouse serum; *NR*, non-reduced.

R1 inhibits Merozoite Invasion by Preventing the Association between PfAMA1 and the PfRON Complex—It has been shown recently that the 4G2 anti-PfAMA1 invasion inhibitory antibody, which binds on one side of the conserved hydrophobic trough, fails to immunoprecipitate the RON complex, suggesting that this region of PfAMA1 was involved in this interaction. Experiments using PfAMA1 alleles mutagenized in the hydrophobic pocket further supported this conclusion (16). Having demonstrated that the R1 peptide also binds to the hydrophobic trough of PfAMA1, we reasoned that this may prevent the formation of the PfAMA1-PfRON complex. To investigate this possibility, we took advantage of the fact that binding of PfAMA1 to the PfRON complex occurs in solution, after lysis of schizont stage parasites, so by performing the lysis in the presence of the R1 peptide, we could potentially block this interaction. As shown in Fig. 4*A*, *panels i* and *ii*, increasing the amount of R1 peptide in the lysis buffer resulted in a dose-dependent decrease in the amount of PfRON4 and PfRON5 immunoprecipitated by an anti-PfAMA1 antibody. To confirm that this decrease was not related to a concomitant inhibition of PfAMA1 binding by its antibody, eluates were probed with anti-PfAMA1. As shown in Fig. 4*A*, *panel* iii, increasing quantities of R1 had no effect on the amount of PfAMA1 immunoprecipitated. Moreover, increasing concentrations of an unrelated peptide (*X1*) had no effect on the PfAMA1-RON association, demonstrating that the inhibition is specific to R1 (Fig. 4*A*, *panels iv* and *v*). Absolute quantification of the amount of each protein immunoprecipitated under the different conditions is not biologically signif-

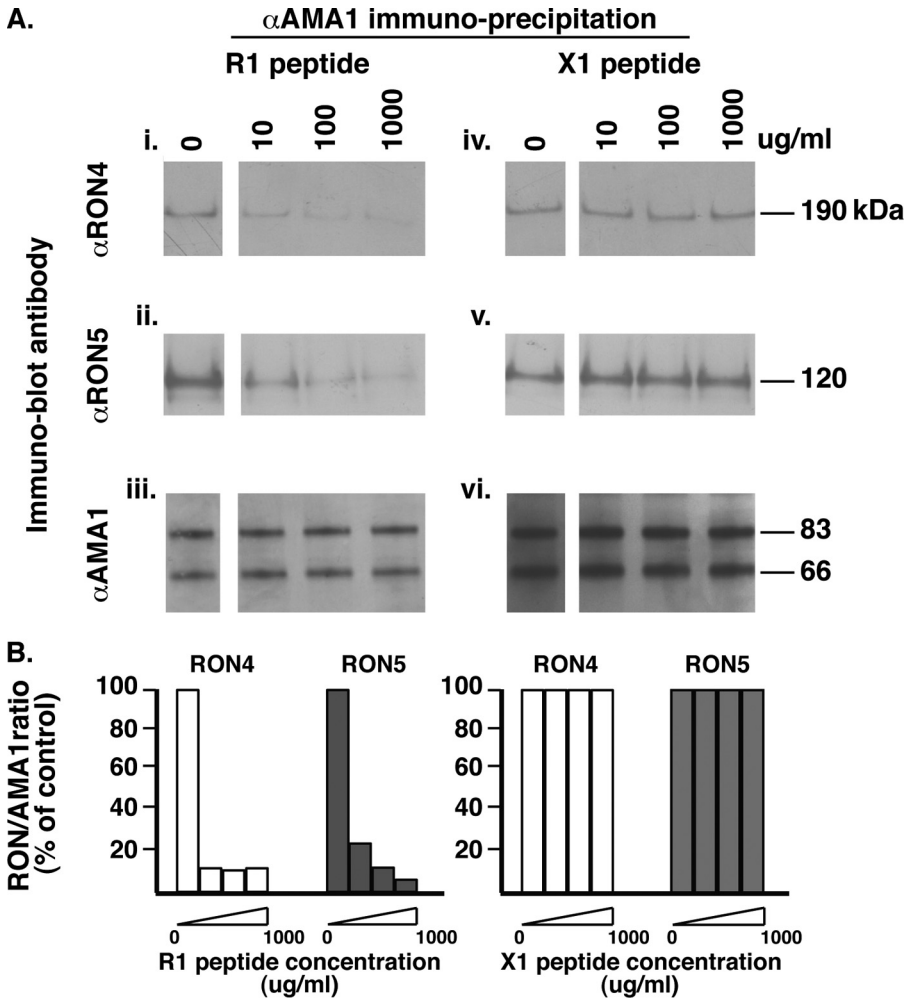

FIGURE 4. **R1 prevents the association between PfAMA1 and the PfRON complex.** *A*, PfAMA1 immunoprecipitation on schizont stage parasites solubilized in increasing concentrations of the R1 peptide shows a dose-dependent decrease in the amount of PfRON4 and PfRON5 pulled down. An unrelated peptide (*X1*) does not have any effect on the PfAMA1-RON interaction. *B*, relative amounts of each RON pulled down by AMA1 under increasing amounts of R1 or X1 peptide.

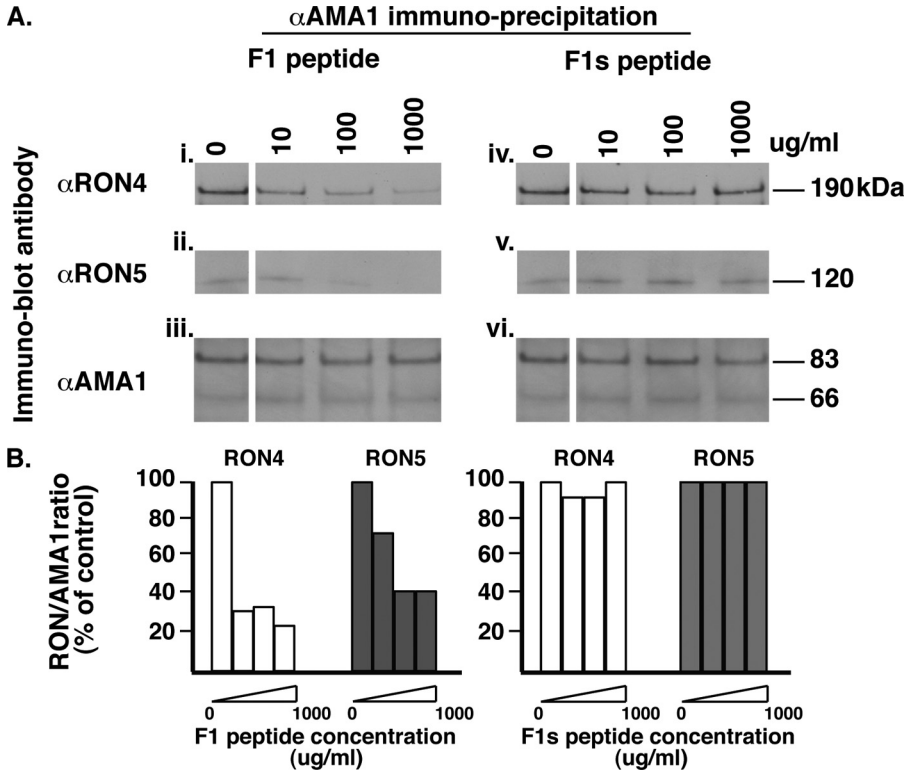

FIGURE 5. **F1 prevents the association between PfAMA1 and the PfRON complex.** *A*, PfAMA1 immunoprecipitation on schizont stage parasites solubilized in increasing concentrations of the F1 peptide shows a dose-dependent decrease in the amount of PfRON4 and PfRON5 pulled down. A scrambled version of F1 (F1s) does not have any effect on the PfAMA1-RON interaction. *B*, relative amounts of each RON pulled down by AMA1 under increasing amounts of F1 or F1s peptide.

icant because of the different efficiencies with which each antibody immunoprecipitates its target protein. We therefore expressed the data as a ratio of the amount of the PfRONs *versus* PfAMA1 immunoprecipitated under each condition tested and the percentage of the PfRON-PfAMA1 ratio obtained without peptide in the lysis buffer (assigned as 100%). This clearly shows that increasing amounts of R1 decrease the amount of both PfRON proteins associated with PfAMA1 (Fig. 4*B*), demonstrating that binding of this inhibitory molecule to the PfAMA1 hydrophobic trough prevents the formation of the tight junction complex. This is consistent with results previously obtained with the 4G2 anti-AMA1 invasion inhibitory antibody (16). Earlier studies had shown that the R1 peptide competed with another invasion inhibitory peptide (F1) for AMA1 binding, leading to the suggestion that both targeted the same binding hot spot on the molecule (19, 35). To verify that the F1 peptide also had the ability to prevent the AMA1-RON interaction, increasing amounts were used in place of R1 in immunoprecipitation assays. As shown in Fig. 5, F1 does decrease the amount of RON4 and RON5 pulled down by the anti-AMA1, although with less efficiency than R1 (Fig. 5*B*); this could explain why the latter is five times more efficient at inhibiting invasion. A scrambled version of the F1 peptide (F1s) (36) failed to prevent the formation of the complex, demonstrating the specificity of inhibition.

DISCUSSION

Invasion of erythrocytes by the malaria parasite *P. falciparum* is an obligatory step during blood stage infection, involving a cascade of molecular events between the parasite and host erythrocyte. We have shown that two distinct peptides that inhibit this process, R1 and F1, both act by blocking the interaction between PfAMA1 and the RON complex, as does the inhibitory antibody 4G2 (30). This is therefore an important and apparently general mechanism of action of inhibitory agents that target AMA1 and represents a viable strategy for new therapeutic agents. A detailed structural understanding of these interactions is therefore of the utmost importance. Although it had been inferred previously that these inhibitory interactions may be localized at the conserved hydrophobic trough of AMA1 (7), we now present direct evidence confirming this localization. Moreover, the NMR probes utilized here should be valuable in further studies of agents targeting this AMA1-RON interaction. A potential drawback of these inhibitory peptides as models for the development of antimalarial drugs is their strain specificity, but we have shown recently that relatively simple modifications of R1 can enhance its affinity for AMA1 from the strains HB3 and W2mef (20). This, together with the apparently conserved nature of the AMA1 hydrophobic trough and the AMA1-RON interaction, strongly suggests that strain-independent inhibition should be achievable by this mechanism. Videomicroscopy of merozoites invading erythrocytes has provided an overall view of the process that can now be used as a framework to dissect the mechanisms involved at each step (2, 21) (supplemental Fig. 2*A*). The results presented here are a first step in this direction.

P. falciparum merozoites incubated in the presence of R1 proceed from initial contact with the erythrocyte through to the reorientation and formation of the tight junction between the apical tip of the parasite and the red blood cell membrane (21) (supplemental Fig. 2*B*, *red arrows*). The merozoite can then be seen to pull on the red blood cell, causing it to wrap around the apical tip, but invasion fails to proceed (supplemental Fig. 2*B*, *yellow arrows*, *24.1 s*). This suggests that the machinery required by the parasite to propel itself, that is, adhesin binding and actomyosin motor engagement, is established and functional, with its action pushing the merozoite against the erythrocyte membrane. This, combined with our data demonstrating that R1 blocks PfAMA1 function by preventing its association with the PfRON complex, allows us to precisely define the step at which this interaction takes place during the invasion process, *i.e.* after reorientation and establishment of the initial tight junction and motor engagement (Fig. 6). We thus hypothesize that the interaction of PfAMA1 with the

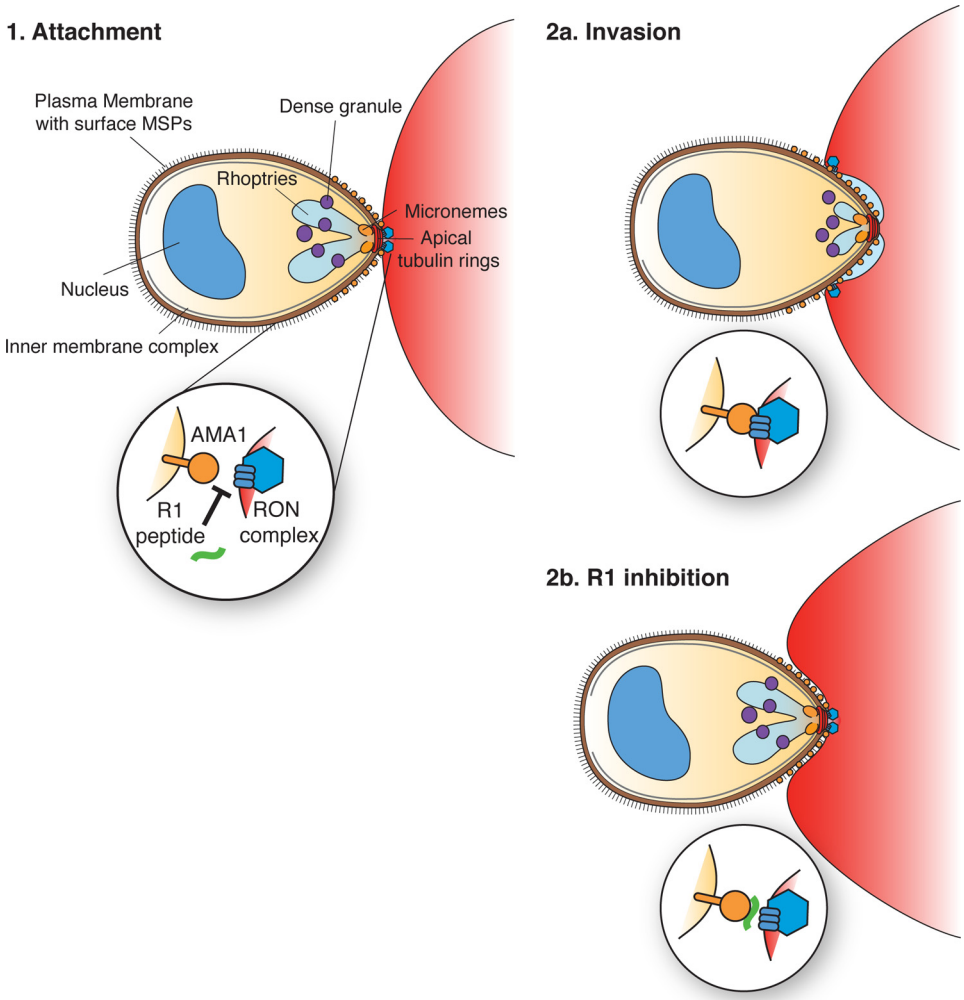

FIGURE 6. **A model for the early step of merozoite invasion of erythrocytes.** *1*, after initial contact and reorientation of the merozoite, its apical tip comes in contact with the erythrocyte membrane, leading to the formation of a tight junction and translocation of the RON complex across the host cell membrane. *2a*, interaction between the RON complex and AMA1 triggers secretion of the rhoptry bulb contents, which are then used in the generation of the nascent parasitophorous vacuole. The parasite can then pull itself through the tight junction powered by its actomyosin motor. *2b*, binding of the R1 peptide to the AMA1 hydrophobic trough prevents its interaction with the RON complex and subsequent rhoptry secretion. However, because the tight junction and the invasion motor are established, the merozoite is able to pull on the red blood cell, which ends up wrapping around the parasite because of the absence of a nascent parasitophorous vacuole. *MSPs* refers to merozoite surface proteins.

PfRONs results in the secretion of the rhoptries, whose contents likely form the nascent parasitophorous vacuole membrane, and that R1 inhibits invasion by preventing the steps that initiate secretion of the rhoptry bulb contents. Recent work in *T. gondii* has shown that the TgRON complex was translocated into the host cell cytosol, with TgRON2 spanning the host plasma membrane and acting as a receptor for TgAMA1 (37, 38). Whether this is also true for *Plasmodium* is not known at the moment but, if this is the case, we believe that R1 inhibition would occur subsequently to this translocation and therefore that secretion of the rhoptry neck requires different signals than the ones involved in rhoptry bulb secretion. Earlier studies have shown that rhoptries contain high amounts of lamellar deposits, most likely made up of lipids (39, 40), which are predicted to be released at the point of contact between the invading merozoite and the red blood cell (41). In untreated parasites, following the formation of the junction aperture, release of the rhoptry contents allows for the generation of the nascent parasitophorous vacuole, which then most likely provides necessary space for the merozoite to push through as the actomyosin motor propels it forward (39). Electron micrograph images of invading *Plasmodium knowlesi* merozoites, treated with cytochalasin B (which blocks actin filament polymerization but not tight junction formation), reveal the presence of vesicles in the red blood cell cytoplasm at the point of contact between the apical tip of the parasite and the erythrocyte membrane, suggesting that blocking motor function, although arresting invasion, does not prevent rhoptry secretion (42). We predict that R1-treated *P. falciparum* parasites would not show these vesicles, as precursors to full rhoptry release. Unfortunately, capturing *P. falciparum* merozoites mid-invasion is a very rare event because of the fragile nature of merozoites from this species and has not as yet been documented by electron microscopy.

The fact that the AMA1-RON complex interaction has been observed in other *Plasmodium* species (43, 44) and *T. gondii* (13) suggests a conserved mechanism of rhoptry release across apicomplexan parasites. Indeed, a *T. gondii* strain with a conditional knock-out of TgAMA1 fails to invade and was shown to be defective in rhoptry secretion (45). A role for AMA1 in rhoptry secretion is further supported by its absence in the ookinete stage, which does not have rhoptries (46). This highlights the signals that link binding of AMA1 to the RONs, and subsequent rhoptry secretion, as key areas of future study. A recent report demonstrating the importance of phosphorylated residues in the PfAMA1 cytoplasmic tail to invasion provides a tantalizing possibility for the mechanism behind this signaling event (21).

Acknowledgments—We thank Tony Triglia and Wai-Hong Tham for critical reading of the manuscript. We also thank the Red Cross Blood Service (Melbourne, Australia) for supply of red cells and serum.

REFERENCES

1. Cowman, A. F., and Crabb, B. S. (2006) *Cell* **124,** 755–766
2. Gilson, P. R., and Crabb, B. S. (2009) *Int. J. Parasitol.* **39,** 91–96
3. Dvorak, J. A., Miller, L. H., Whitehouse, W. C., and Shiroishi, T. (1975)

Science **187,** 748–750
4. Aikawa, M. (1977) *Bull. World Health Organ.* **55,** 139–156
5. Aikawa, M., Miller, L. H., Johnson, J., and Rabbege, J. (1978) *J. Cell Biol.* **77,** 72–82
6. Aikawa, M., Miller, L. H., Rabbege, J. R., and Epstein, N. (1981) *J. Cell Biol.* **91,** 55–62
7. Harris, P. K., Yeoh, S., Dluzewski, A. R., O'Donnell, R. A., Withers-Martinez, C., Hackett, F., Bannister, L. H., Mitchell, G. H., and Blackman, M. J. (2005) *PLoS Pathog.* **1,** 241–251
8. Bannister, L. H., Mitchell, G. H., Butcher, G. A., Dennis, E. D., and Cohen, S. (1986) *Cell Tissue Res.* **245,** 281–290
9. Langreth, S. G., Jensen, J. B., Reese, R. T., and Trager, W. (1978) *J. Protozool.* **25,** 443–452
10. Triglia, T., Healer, J., Caruana, S. R., Hodder, A. N., Anders, R. F., Crabb, B. S., and Cowman, A. F. (2000) *Mol. Microbiol.* **38,** 706–718
11. Mitchell, G. H., Thomas, A. W., Margos, G., Dluzewski, A. R., and Bannister, L. H. (2004) *Infect. Immun.* **72,** 154–158
12. Lebrun, M., Michelin, A., El Hajj, H., Poncet, J., Bradley, P. J., Vial, H., and Dubremetz, J. F. (2005) *Cell Microbiol.* **7,** 1823–1833
13. Alexander, D. L., Mital, J., Ward, G. E., Bradley, P., and Boothroyd, J. C. (2005) *PLoS Pathog.* **1,** e17
14. Alexander, D. L., Arastu-Kapur, S., Dubremetz, J. F., and Boothroyd, J. C. (2006) *Eukaryot. Cell* **5,** 1169–1173
15. Cao, J., Kaneko, O., Thongkukiatkul, A., Tachibana, M., Otsuki, H., Gao, Q., Tsuboi, T., and Torii, M. (2009) *Parasitol. Int.* **58,** 29–35
16. Collins, C. R., Withers-Martinez, C., Hackett, F., and Blackman, M. J. (2009) *PLoS Pathog.* **5,** e1000273
17. Morahan, B. J., Sallmann, G. B., Huestis, R., Dubljevic, V., and Waller, K. L. (2009) *Exp. Parasitol.* **122,** 280–288
18. Hodder, A. N., Crewther, P. E., and Anders, R. F. (2001) *Infect. Immun.* **69,** 3286–3294
19. Harris, K. S., Casey, J. L., Coley, A. M., Masciantonio, R., Sabo, J. K., Keizer, D. W., Lee, E. F., McMahon, A., Norton, R. S., Anders, R. F., and Foley, M. (2005) *Infect. Immun.* **73,** 6981–6989
20. Harris, K. S., Casey, J. L., Coley, A. M., Karas, J. A., Sabo, J. K., Tan, Y. Y., Dolezal, O., Norton, R. S., Hughes, A. B., Scanlon, D., and Foley, M. (2009) *J. Biol. Chem.* **284,** 9361–9371
21. Treeck, M., Zacherl, S., Herrmann, S., Cabrera, A., Kono, M., Struck, N. S., Engelberg, K., Haase, S., Frischknecht, F., Miura, K., Spielmann, T., and Gilberger, T. W. (2009) *PLoS Pathog.* **5,** e1000322
22. Trager, W., and Jensen, J. B. (1976) *Science* **193,** 673–675
23. Lambros, C., and Vanderberg, J. P. (1979) *J. Parasitol.* **65,** 418–420
24. Gupta, A., Bai, T., Murphy, V., Strike, P., Anders, R. F., and Batchelor, A. H. (2005) *Protein Expr. Purif.* **41,** 186–198
25. Muchmore, D. C., McIntosh, L. P., Russell, C. B., Anderson, D. E., and Dahlquist, F. W. (1989) *Methods Enzymol.* **177,** 44–73
26. Topolska, A. E., Lidgett, A., Truman, D., Fujioka, H., and Coppel, R. L. (2004) *J. Biol. Chem.* **279,** 4648–4656
27. Healer, J., Murphy, V., Hodder, A. N., Masciantonio, R., Gemmill, A. W., Anders, R. F., Cowman, A. F., and Batchelor, A. H. (2004) *Mol. Microbiol.* **52,** 159–168
28. Rug, M., Wickham, M. E., Foley, M., Cowman, A. F., and Tilley, L. (2004) *Infect. Immun.* **72,** 6095–6105
29. Coley, A. M., Gupta, A., Murphy, V. J., Bai, T., Kim, H., Foley, M., Anders, R. F., and Batchelor, A. H. (2007) *PLoS Pathog.* **3,** 1308–1319
30. Collins, C. R., Withers-Martinez, C., Bentley, G. A., Batchelor, A. H., Thomas, A. W., and Blackman, M. J. (2007) *J. Biol. Chem.* **282,** 7431–7441
31. Ossorio, P. N., Schwartzman, J. D., and Boothroyd, J. C. (1992) *Mol. Biochem. Parasitol.* **50,** 1–15
32. Howard, R. F., Stanley, H. A., Campbell, G. H., and Reese, R. T. (1984) *Am. J. Trop. Med. Hyg.* **33,** 1055–1059
33. Bushell, G. R., Ingram, L. T., Fardoulys, C. A., and Cooper, J. A. (1988) *Mol. Biochem. Parasitol.* **28,** 105–112
34. Howard, R. F., and Reese, R. T. (1990) *Exp. Parasitol.* **71,** 330–342
35. Li, F., Dluzewski, A., Coley, A. M., Thomas, A., Tilley, L., Anders, R. F., and Foley, M. (2002) *J. Biol. Chem.* **277,** 50303–50310
36. Keizer, D. W., Miles, L. A., Li, F., Nair, M., Anders, R. F., Coley, A. M., Foley, M., and Norton, R. S. (2003) *Biochemistry* **42,** 9915–9923
37. Straub, K. W., Cheng, S. J., Sohn, C. S., and Bradley, P. J. (2009) *Cell Microbiol.* **11,** 590–603
38. Besteiro, S., Michelin, A., Poncet, J., Dubremetz, J. F., and Lebrun, M. (2009) *PLoS Pathog.* **5,** e1000309
39. Bannister, L. H., Mitchell, G. H., Butcher, G. A., and Dennis, E. D. (1986) *Parasitology* **92,** 291–303
40. Stewart, M. J., Schulman, S., and Vanderberg, J. P. (1986) *Am. J. Trop. Med. Hyg.* **35,** 37–44
41. Bannister, L. H., and Mitchell, G. H. (1989) *J. Protozool.* **36,** 362–367
42. Miller, L. H., Aikawa, M., Johnson, J. G., and Shiroishi, T. (1979) *J. Exp. Med.* **149,** 172–184
43. Narum, D. L., Nguyen, V., Zhang, Y., Glen, J., Shimp, R. L., Lambert, L., Ling, I. T., Reiter, K., Ogun, S. A., Long, C., Holder, A. A., and Herrera, R. (2008) *Infect. Immun.* **76,** 4876–4882
44. Narum, D. L., Ogun, S. A., Batchelor, A. H., and Holder, A. A. (2006) *Infect. Immun.* **74,** 5529–5536
45. Mital, J., Meissner, M., Soldati, D., and Ward, G. E. (2005) *Mol. Biol. Cell* **16,** 4341–4349
46. Lal, K., Prieto, J. H., Bromley, E., Sanderson, S. J., Yates, J. R., 3rd, Wastling, J. M., Tomley, F. M., and Sinden, R. E. (2009) *Proteomics* **9,** 1142–1151